



Numerical simulation for the steam gasification of single char particle

Vinod Kumar Yadav^{1,2} · Ravi Shankar³ · Vineet Kumar^{2,4}

Received: 13 May 2020 / Accepted: 9 September 2020 / Published online: 15 September 2020
© Institute of Chemistry, Slovak Academy of Sciences 2020

Abstract

Simulation of a single char particle for the synthesis gas production is challenging task due to its complex chemical reactions coupled with the varying physicochemical properties during the gasification process. Steam gasification of a single char particle require the favourable conditions for the CO and H₂ enriched gas with minimum CO₂ formation. Here, non-linear partial differential equation for the unsteady state diffusion-controlled reaction of a gasification agent (steam) inside the non-catalytic porous spherical char particle is numerically solved by staggered grid finite volume method with suitable boundary conditions. The steam gasification is numerically solved for the variable size char particle of two different diameters, i.e. 5 and 10 mm between the temperature range of 1000–1300 K. Gasification process at high-steam partial pressure suggests high H₂ and CO concentration in the synthesis gases.

Keywords Coal · Gasification · Steam · Staggered grid · Finite volume method (FVM)

Introduction

Coals from different regions of the world have different characteristics in term of mineral content and carbon matrix. In high ash containing coals, beneficiation process is difficult for the mineral matter removal that leads to the lower efficiency and greater environmental pollution during coal combustion. The carbon dioxide emissions from the coal combustion leads to global warming that has led to the international agreement that sets the target for controlling CO₂ emissions. To achieve these goals, it is required to enhance

the energy efficiency by making changes in the combustion practices of solid fuel.

In many countries, the coal reserves are in better condition than oil and natural gas (Chavan et al. 2012). Owing to this reason, countries like India, using coal-based energy option for their economy and approximately 70–80% of energy are based on the thermal (coal) power plants (Choudhary and Shankar 2012). These power plants unit generate considerable amount of CO₂, which is responsible for major environmental pollution (Chandra and Chandra 2004). Although liquid and gaseous fuel produce less pollutants and require less transportation/operational cost in comparison with the solid fuels (Mohamad 2005). Hence, conversion of these solid fuel to liquid/gaseous fuel could be the better option for less pollution generation. There are many theory/methods related to solid (coal/char) to liquid/gaseous fuel conversion are already available in the literature (Varma et al. 2019). In this constituent, char gasification has been a subject of international interest for many years. Char gasification is commercially important not only for energy production but also its applications in the production of synthesis gas, ammonia, hydrogen, methanol and various other purposes.

Gasification of char is one of the effective energy conversion methods for the utilization of coal to produce gaseous fuel (Umeki et al. 2010) and high fraction of combustible gas is preferred for wider application during gasification process,

Electronic supplementary material The online version of this article (<https://doi.org/10.1007/s11696-020-01348-2>) contains supplementary material, which is available to authorized users.

✉ Ravi Shankar
bits.iitr@gmail.com

- ¹ Department of Chemical Engineering, Government Polytechnic Gorakhpur, Gorakhpur, Uttar Pradesh 273012, India
- ² Department of Chemical Engineering, Indian Institute of Technology Roorkee, Roorkee, Uttarakhand 247667, India
- ³ Department of Chemical Engineering, Madan Mohan Malaviya University of Technology Gorakhpur, Gorakhpur, Uttar Pradesh 273016, India
- ⁴ Department of Chemical Engineering, Indian Institute of Technology (ISM) Dhanbad, Dhanbad 826004, India

the use of steam as a gasification agent appears to be excellent options, due to the absence of nitrogen. Also, the steam gasification has higher reactivity responsible for higher composition of H₂ and CO in the product gases (Gomez and Mahinpey 2015; Jayaraman et al. 2017; Shufen and Ruizheng 1994; Tremel and Spliethoff 2013; Wang et al. 2016; Ye et al. 1998). The effects of composition of gasification agent on the rate of gasification of char have been discussed by many researchers (Everson et al. 2006; Kwon et al. 1988) and it is reported that the rate of the gasification increases with increase in the concentration of gasification agent. The size of the char particle also affects the rate of gasification process. Because large particle has less surface area than the smaller one and the rate of conversion into gaseous product is higher for the smaller particle (Kajitani et al. 2006; Luo et al. 2001). This variation in the conversion rate with the char particle size is also due to the internal effects such as, molecular diffusion, availability of oxygen. The reaction temperature is expected to be another most important operating variable affecting the performance of a gasification process. Since the main gasification reactions are endothermic and increase in temperature favours higher conversion. In carbon-steam reaction-based gasification process, generated gaseous product contains CO and H₂ as a major composition and its concentration can be enhanced by converting unwanted CO₂ to CO at higher temperature according to Boudouard reaction mechanism (Yadav and Kumar 2014). Overall, gasification temperature is crucial parameters in the gasification process and it can be categorised into two parts, at lower temperature, kinetic control prevails for chars, while at higher temperature, diffusional effects (pore diffusion) become dominant and affect the overall reaction rates (Chen et al. 2019; Prabhakar et al. 2019; Zhu et al. 2020). Overall, there are considerable literatures available related to experimental study of steam gasification process, but the simulation approach to study the gasification process is rare in the literature.

The present study deals the quantitative analysis of partial pressure, temperature, molecular diffusivity, char conversion and product formation during the gasification of char particle. MATLAB 2010 are used to solve the different modelled equation. The char particle with porosity 73%, solid and bulk densities 1900 and 507 kg/m³, respectively are used for the gasification process. The gasification-based data of Mermoud et al. (2006) is used for the validation purposes (Mermoud et al. 2006).

Model development

The model introduced to predict the gasification of single spherical char particle during the processing. Following commonly assumed conditions are adopted in the development of the model:

- No solid products other than ash is form during the reactions.
- There is no volatile material and moisture in the char particle.
- Constant total pressure inside the char particle.
- No change in particle size during reactions.
- Isothermal condition.
- Variation of particle porosity during its gasification process depends only on the carbon composition.

The current models consider only gasification after the pyrolysis process and first two assumptions are considered. During the pyrolysis operation ash as well as volatile content are not considered while temperature and pressure vary inside the char particle. Less variation in these two parameters may be noted due to small size of char particle, due to this reason these assumption are incorporated.

Material balance for gaseous species

Mathematical modelling for the steam gasification of a single char particle involves the mole balances over a small spherical volume element of thickness Δr having radius ‘ r ’, during the time interval t and $t + \Delta t$. The concentration of various species at nodes represented by C_i (Fig. 1) and molar flux was calculated across the boundaries of volume elements represented by r_i in the same Fig. 1. Where ‘ i ’ was varied from 1 to N .

Performing a molar balance for the gasification agent (H₂O) and product gas, C_{ji} (H₂, CO, CO₂ and CH₄) at any time ‘ t ’ over the i th volume element bounded between radius r_{i-1} and r_i (Fig. 1) can be presented as Eq. (1) using the staggered grid finite volume method (SGFVM):

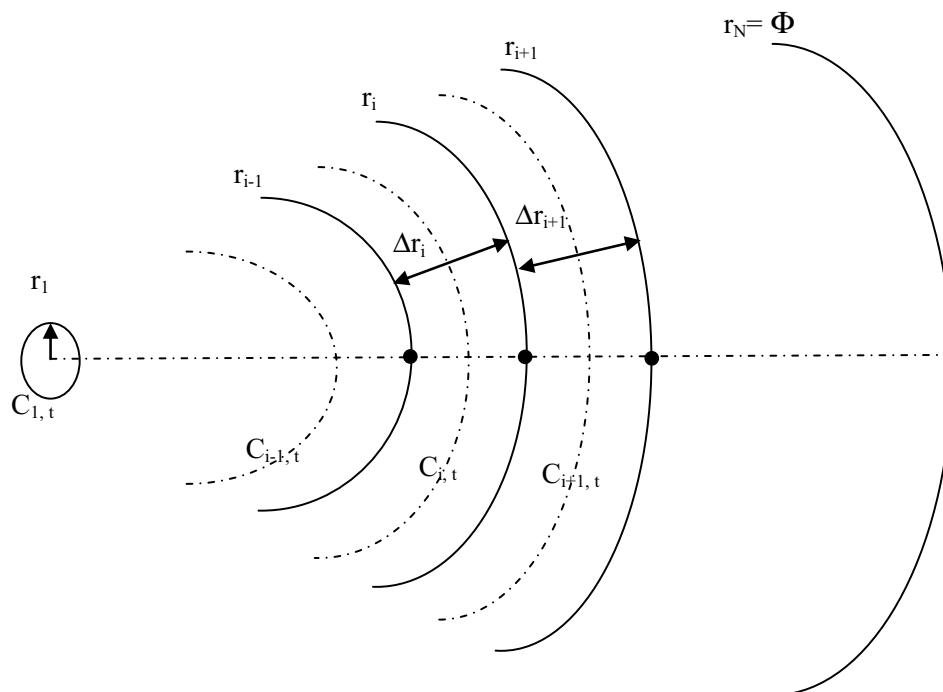
$$\frac{2r_i^2 D_{ej(i+1)} (C_{j(i+1),t} - C_{ji,t})}{(\Delta r_i + \Delta r_{i+1})} - \frac{2r_{i-1}^2 D_{eji} (C_{ji,t} - C_{j(i-1),t})}{(\Delta r_i + \Delta r_{i+1})} = \frac{1}{3} (r_i^3 - r_{i-1}^3) \left[\frac{C_{ji,t+\Delta t} - C_{ji,t}}{\Delta t} - R_{ji,t} \right]. \quad (1)$$

Rearranging Eq. (1), the following recurrence Eq. (2) is obtained:

$$C_{ji,t+\Delta t} = (C_{ji,t} + R_{ji,t} \Delta t) + \frac{6}{(r_i^3 - r_{i-1}^3)} \left[\frac{r_i^2 D_{ej(i+1)} (C_{j(i+1),t} - C_{ji,t})}{(\Delta r_i + \Delta r_{i+1})} - \frac{r_{i-1}^2 D_{eji} (C_{ji,t} - C_{j(i-1),t})}{(\Delta r_i + \Delta r_{i-1})} \right] \Delta t, \quad (2)$$

where D_{eji} is the effective diffusivity of j th component in the i th element at time t . C_j is the concentration of j th species which are H₂O, H₂, CO, CO₂ and CH₄ at the same time. The term $R_{ji,t}$ is a function of concentration which is based on the reaction rate of the species.

Fig. 1 Spherical volume elements inside the char particle



Equation (2) can be solved for the j th species using the following boundary conditions (B.C.) (Yadav and Kumar 2016):

B.C.I : at $t = 0$, $C_j = 0$

(for all r , and $j = \text{H}_2\text{O}, \text{H}_2, \text{CO}, \text{CO}_2, \text{CH}_4$)

B.C.II : at $r = \phi$, $\frac{\partial C_j}{\partial r} = 0$ (for all t , and j)

B.C.III : at $r = 0$, $\frac{\partial C_j}{\partial r} = 0$ (for all t , and j).

Performing a molar balance for j th species at centre of the coal char particle, Eq. (1) can be reduced to Eq. (3):

$$C_{j1,t+\Delta t} = (C_{j1,t} + R_{j1,t}\Delta t) + 6D_{ej1,t} \left[\frac{(C_{j2,t} - C_{j1,t})}{r_1(\Delta r_1 + \Delta r_2)} \right] \Delta t. \tag{3}$$

The value of $R_{j1,t}$ (function of concentration) is based on the rate of reactions of the j th species at the centre of the particle. Here it is noted that for the central volume element, radius $r_1 = \Delta r_1$ and in all the elements R_j is negative for reactant (H_2O) and positive for products ($\text{H}_2, \text{CO}, \text{CO}_2$ and CH_4) in Eqs. (2) and (3).

Material balance for solid reactant (carbon)

Performing a molar balance for the carbon over the i th volume element bounded between r_{i-1} and r_i (Fig. 1) in the same way as discussed above, as Eq. (4):

$$-\frac{\partial C_C}{\partial t} \Big|_{C_{Ci}} = -R_{Ci,t} \tag{4}$$

The rate of consumption of carbon, $-R_{Ci,t}$ is a function of the concentration of carbon and other reactants in the i th volume element.

Using SGFVM approach, the recurrence equation for carbon can be written as Eq. (5):

$$C_{Ci,t+\Delta t} = C_{Ci,t} + R_{Ci,t}\Delta t, \tag{5}$$

the following boundary condition can be used for carbon gasification:

B.C.IV : at $t = 0$, $C_C = C_{C0}$ (for all r).

Variation of porosity and effective diffusivity

Pore structure of char is a factor which controls the gasification reaction rate. Although it is not a controlling factor for highly reactive chars (Mishra et al. 2018). The porosity and the internal structure of char particle changes considerably

during the gasification and it is also affecting the other properties, such as molecular diffusivity. Since the porosity of the char particle is linearly dependent on the carbon content, the following Eq. (6) can be used for predicting porosity changes during reactions (Gil et al. 2011):

$$\varepsilon_p = \varepsilon_0 + X(1 - \varepsilon_0), \quad (6)$$

where ε_0 is the initial char particle porosity and X is the fractional conversion of the char particle given by Eq. (7):

$$X = 1 - \frac{m(t)}{m_0}, \quad (7)$$

where m_0 is the initial mass of particle (initial mass of carbon and ash) and $m(t)$ is the mass of particle (mass of carbon and ash) at any time t ($t > 0$).

Equation (8) has been used by many researchers (Gomez-Barea and Ollero 2006; Holikova et al. 2005; Zajdlík et al. 2001) to correlate effective diffusivity in terms of increment in porosity and the initial diffusivity:

$$\frac{D_{ej}}{D_{ej}^0} = \left(\frac{\varepsilon_p}{\varepsilon_0} \right)^\infty, \quad (8)$$

where ∞ is equal to 2 for random pore size distribution and D_{ej}^0 is the initial effective diffusivity of j th components in solid phase.

Kinetics of char gasification

Five kinetics mechanism, steam gasification (R1), hydrogasification (methanation) (R2), boudouard reaction (R3), methane steam reforming (R4) and water gas shift reaction (R5) are used for the char gasification process and represented

in Table 1. The modelling, simulation and kinetic of char gasification studies have been carried out by many researchers using different combinations of these reactions and their respective rate kinetics (Groeneveld and Swaij 1980; Mendes et al. 2008; Corella and Sanz 2005; Inayat et al. 2010).

The overall volumetric rate of generation of each j th component, R_j ($= \partial C_j / \partial t$), as presented in Table 1, can be represented as Eqs. (9–13):

$$R_{H_2O} = \frac{\partial C_{H_2O}}{\partial t} = -r_1 - r_4 - r_5 \quad (9)$$

$$R_{H_2} = \frac{\partial C_{H_2}}{\partial t} = r_1 + 3r_4 + r_5 - 2r_2 \quad (10)$$

$$R_{CO} = \frac{\partial C_{CO}}{\partial t} = r_1 + 2r_2 + r_4 - r_5 \quad (11)$$

$$R_{CH_4} = \frac{\partial C_{CH_4}}{\partial t} = r_2 - r_4 \quad (12)$$

$$R_{CO_2} = \frac{\partial C_{CO_2}}{\partial t} = -r_3 + r_5. \quad (13)$$

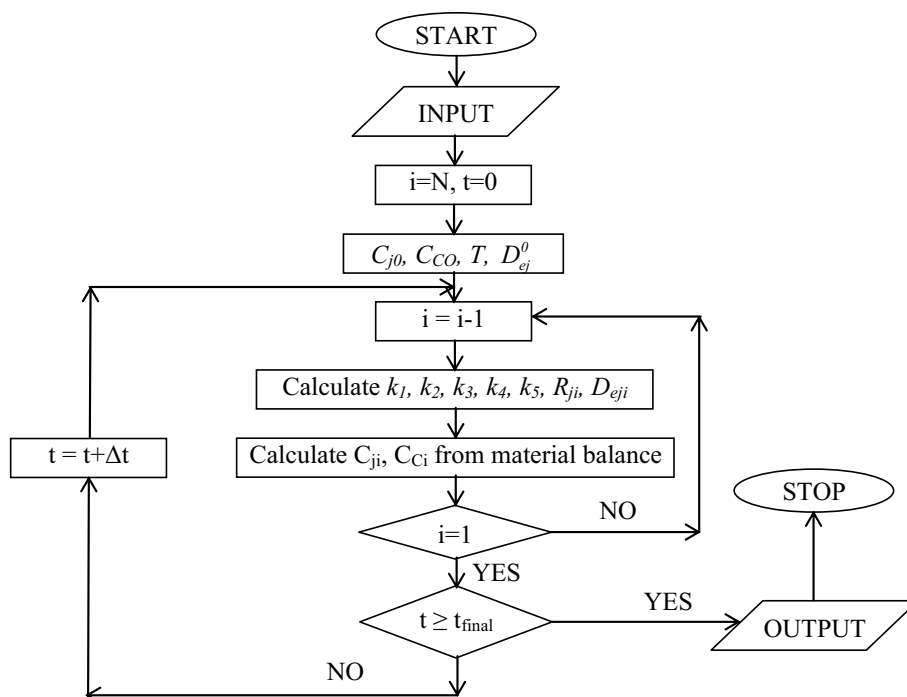
Calculation procedure

The flow diagram for the overall solution in the MATLAB program is shown in Fig. 2. In this algorithm, solution begins with assigning variables and applying appropriate boundary conditions at $t=0$. Then concentration and reaction rate are calculated sequentially beginning from particle

Table 1 Steam gasification reactions with kinetic parameters and rate of reaction

Reaction no.	Reaction name	Reaction	Heat of reaction (kJ/mol)	Rate of reaction, $\left(\frac{\text{mole}}{\text{m}^3\text{s}}\right)$	Rate constants	References
R1	Steam gasification	$C + H_2O \rightarrow CO + H_2$	+ 131.4	$r_1 = k_1 C_{\text{char}} C_{H_2O}$	$k_1 = 10^6 \exp\left(-\frac{217100}{RT}\right)$	Groeneveld and Swaij (1980)
R2	Hydro gasification (methanation)	$C + 2H_2 \rightarrow CH_4$	- 75	$r_2 = \frac{6}{d_p} k_2 C_{H_2}$	$k_2 = 2000 \exp\left(-\frac{230274}{RT}\right)$	Mendes et al. (2008)
R3	Boudouard reaction	$C + CO_2 \rightarrow 2CO$	+ 172	$r_3 = k_3 S_{\text{char}} C_{CO_2}^{0.83}$	$k_3 = 7.2 \exp\left(-\frac{2000}{T}\right)$	Corella and Sanz (2005)
R4	Methane steam reforming	$CH_4 + H_2O \rightarrow CO + 3H_2$	+ 206.4	$r_4 = k_4 C_{CH_4} C_{H_2O}$	$k_4 = 3 \times 10^5 \exp\left(-\frac{15000}{T}\right)$	Inayat et al. (2010)
R5	Water gas shift reaction	$CO + H_2O \leftrightarrow CO_2 + H_2$	- 41.7	$r_5 = k_5 \left[\frac{C_{CO} C_{H_2O}}{C_{CO_2} C_{H_2}} - \frac{1}{k_w} \right]$	$k_5 = 10^6 \exp\left(-\frac{6370}{T}\right)$ $k_w = 520 \exp\left(-\frac{7230}{T}\right)$	Corella and Sanz (2005)

d_p diameter (m) of char particle, S_{char} specific surface area of char particle (m^2/m^3)

Fig. 2 Flow diagram for solution of material balance

surface to centre of the particle. Material balance for each volume element at any time t is made for every small-time interval Δt : 0.00001 s and their resulting concentration is predicted at time $t + \Delta t$. The same sequence of calculation is repeated (from particle surface to the centre of the particle) for the regular time interval (Δt) till the final time set for the analysis is attained.

Results and discussion

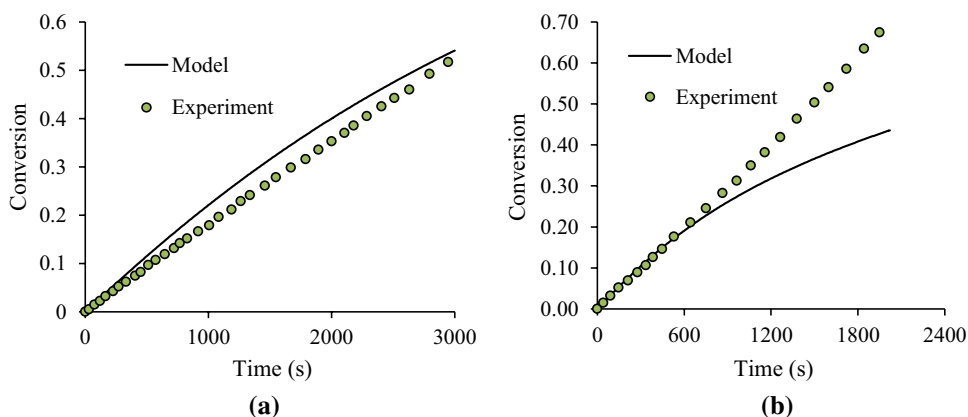
Model validation

The present simulation model is validated with the data of Mermoud et al. (2006) for the single char particle of size

10 mm in term of their conversion with respect to time at two different temperature 1100 and 1200 K and steam pressure 0.2 and 0.1 atm, respectively. The modelled and experimental value of char conversion at both temperatures are represented in Fig. 3a, b, respectively.

It is evident from Fig. 3a that the simulated data are not showing more deviation with experimental data while in Fig. 3b simulated data are showing more deviation with respect to experimental data. At higher temperature, however, predicted result follows experimental values only during initial period of gasification (up to 500 s). After 500 s, the experimental result continues to follow a constant rate of conversion (linear X vs. t plot), but the model results are concave downward. This difference is due to uneven shrinking size of the char particle during gasification of char particle (Mermoud et al. 2006) and the constant size of

Fig. 3 Gasification of charcoal particles at temperature **a** 1100 K, partial pressure 0.2 atm, **b** 1200 K, partial pressure 0.1 atm



spherical char particle assumed in the present model. Owing to this, model predicted rate of conversion decreases with time which is in tune with the observation made by many researchers (Wang et al. 2009; Xu et al. 2011). Further, it is observed that at lower temperature, gasification of a char particle follows progressive reaction model and it is shifted to shrinking core model gradually with increase in temperature (Lahijani et al. 2015). Therefore, at lower temperature, gasification takes place everywhere inside the char particle leading to significant conversion without appreciable change in particle size (i.e. experimental condition remains closer to the model assumption of constant particle size), leading to better match of model result. On the other hand, at higher temperature, change in particle size with conversion is fast (due to shrinking core) that leads to deviation in the experimental and predicted result after 500 s time.

Effect of operating parameters

In the present unsteady state modelling study, the effects of temperature, steam partial pressure, carbon concentration in the char and particle size, during the gasification of char particle on the synthesis gas formation have been studied for the char particle of 5 and 10 mm in the temperature range of 1000–1300 K. It has been observed that conversion increases with operating time at variable operating parameters, which results increase in the porosity of the reacted outer surface of the char particle. Enhanced porosity leading to enhanced effective diffusivity of the steam and products through the outer layer. Overall, the porosity increases from inner surface to outer surface and porosity change causes change in diffusivity, which alters the rate of approach of gasification agent and the rate of removal of products in a complex way. Overall, these phenomena during gasification process may be affected by the variation in the operating factors.

Carbon concentration variation inside char particle

The major reaction in gasification process are endothermic in nature so, gasification process at higher temperature increases the reaction rate inside the char particle. Small char particle size increases the overall surface area and enhances the overall gasification reaction (Hecht et al. 2012). Owing to the molecular diffusion the concentration of the char particle decreases with the radial distance from the char particle. Figure 4 shows carbon concentration inside the particle at different radial distance after 500 s of gasification process at two different temperatures 1000 and 1100 K.

In this study, initial carbon concentration of the solid particle was 260 kmol/m^3 . From Fig. 4, it is evident that at higher temperature (1100 K) carbon concentration remains unchanged up to r/R ratio of 0.5 and then carbon concentration reduces sharply for r/R between 0.5 and 0.7. These

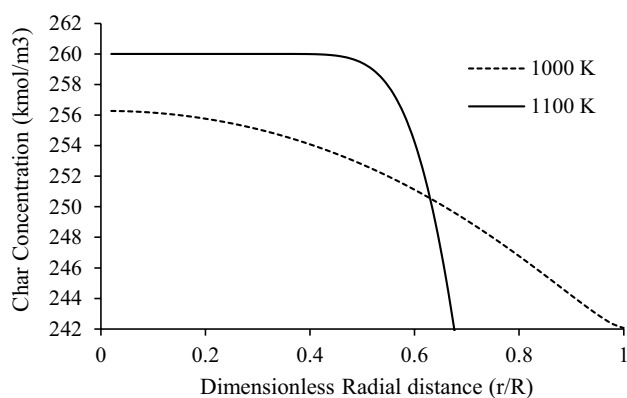


Fig. 4 Effect of char particle size on the reaction mechanism

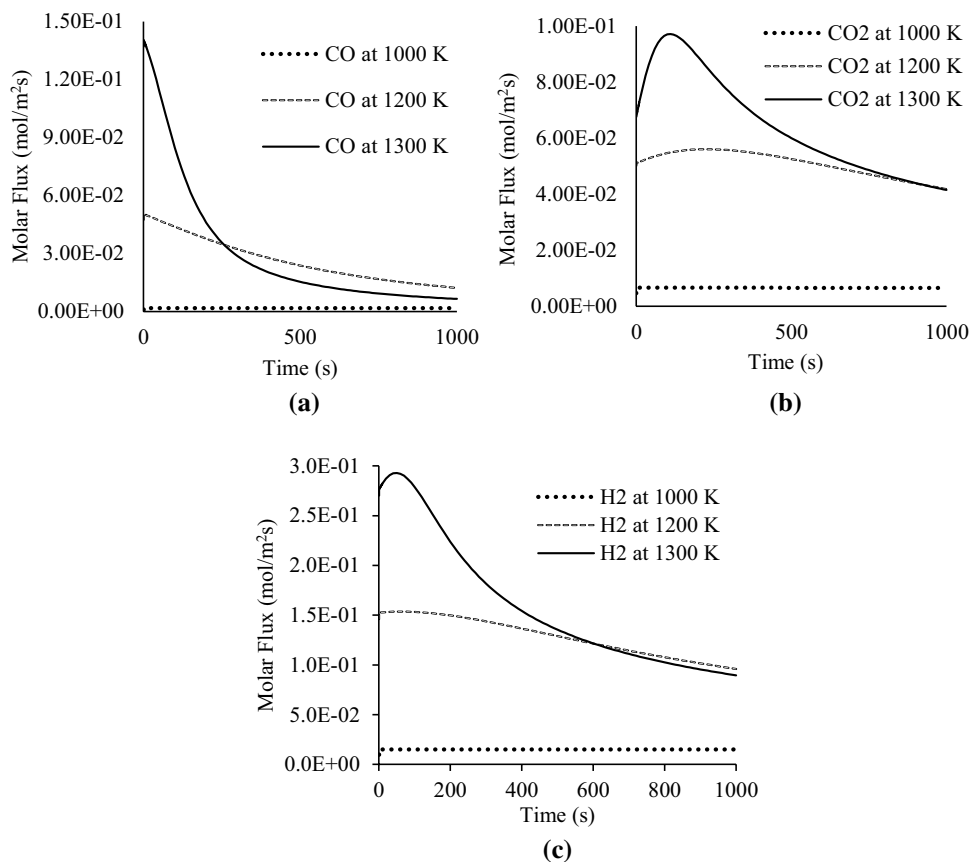
phenomena indicates that the maximum consumption of carbon take place only in this reacting zone as the rate of approach of steam (gasification agent) through the outer ash layer is less than that being consumed in the reacting zone of the particle (Seshadri and Bai 2017). Although gasification process at 1000 K indicates the continuous decrease in carbon concentration with radial distance. This result indicates the rate of reaction becomes low enough to allow the gasification agent to diffuse up to even centre of the particle. Evidently, the gasification reaction follows nearly a shrinking core model when temperature is high and it becomes progressive reaction model at lower temperature (Prabhakar et al. 2019).

Effect of temperature and time on product gases

The rate of consumption of carbon depends not only on the rate of approach of gasification agent but also on the concentration of products, such as hydrogen, carbon dioxide and carbon monoxide (Table 1). Figure 5a–c presents change in molar flux of CO , H_2 and CO_2 coming out of the char particle with the time at three different temperature 1000, 1200 and 1300 K temperature.

From Fig. 5a–c, it is clear that, concentration profiles of various species within the particle changes affect the overall rate of production of gasses at temperature 1200 and 1300 K. Although the rate of production of all the product gasses remains almost constant at the gasification temperature of 1000 K. It is obvious, at the gasification temperature of 1000 K, the reaction rates are slow and steam diffuses deep into the char particle and all the reactions happening simultaneously throughout the particle. Overall, during gasification process, steam gasification reaction (R1) produce enough CO that further reacts with steam through water gas shift reaction (R5) to form CO_2 and H_2 . Thus, although small in amount, but production of all the product species continues for a longer period at almost the same rate.

Fig. 5 Overall molar fluxes of **a** CO, **b** CO₂, **c** H₂ from outer surface of char particle at different temperature (1000, 1200 and 1300 K) and steam partial pressure of 0.1 atm



In the starting of gasification process at 1200 K temperature, the initial rate of formation of CO and CO₂ in the product gas becomes nearly same (Fig. 5a, b). This may be because of the Boudouard reaction (R3) which is favoured at high temperature, producing more CO by consuming generated CO₂ (Li et al. 2020). From Fig. 5, it is also noted that, formation of CO decreases with the gasification time indicating significant conversion through water gas shift reaction (R5) at 1200 K temperature. Upon further increase in temperature up to 1300 K, all the reactions are fast and rate of production of each species are high in the initial phase. However, in the initial phase, maxima of the rate of formation of different species are at different time. It is clear from Fig. 5, that carbon monoxide molar flux start to decline from very beginning of the reaction (after 10 s, if plotted on logarithmic x axis) and CO₂ flux increases up to 100 s due to the water gas shift reaction, but after 100 s CO₂ flux declines because of the rapid formation of ash on the outer surface that reduces the overall rate of reaction. Maximum hydrogen flux is observed at about 50 s and overall mechanism of their formation is varied as CO formation.

The properties of gaseous product can be understood by the CO/CO₂ and H₂/CO ratio. The variation of CO/CO₂ ratio with respect to time is represented in Fig. 6 at three different temperature of 1000, 1200 and 1300 K. Evidently, at lower

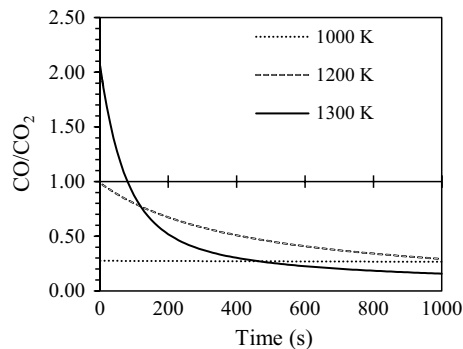


Fig. 6 Overall molar fluxes ratio of CO and CO₂ from outer surface of char particle at different temperature and steam partial pressure of 0.1 atm

temperature, amount of CO produced is always less than CO₂. At higher temperature, i.e. 1300 K, CO production rate is high, but it cannot sustain for longer period. So, at temperature 1300 K, molar flux of CO and CO₂ becomes equal at about 80 s. The H₂/CO ratio during the gasification process is also depends on the gasification temperature and time. The variation of H₂/CO ratio with respect to temperature at 10, 100 and 1000 s are represented in Fig. 7.

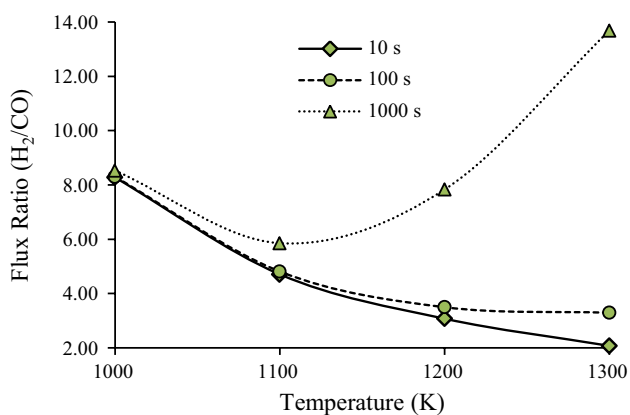


Fig. 7 Overall molar fluxes ratio of H_2 and CO from outer surface of char particle at different time interval with steam partial pressure of 0.1 atm

From Fig. 7 it is noted that, the H_2/CO ratio decreases with the temperature of gasification process while, the H_2/CO ratio at 1000 s decreases from 1000 to 1100 K temperature then increases thereafter.

Because gasification reaction mechanism becomes faster at higher temperature, which is ultimately responsible for higher H_2 production. Although in the starting of gasification process, surface reaction is predominant and hydrogasification and other water shift reaction decreases the H_2 gas in the composition and its ratio also decreases with increase in temperature (Zeng et al. 2015, 2016).

Effect of steam partial pressure

The steam gasification rate of char particle is proportional to the partial pressure of the steam. Figure 8 shows the effect

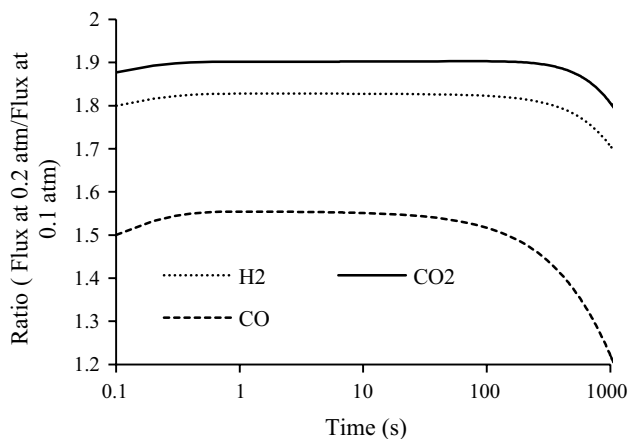


Fig. 8 Ratio of overall molar fluxes of H_2 , CO_2 and CO from outer surface of particle at 0.2 and to 0.1 atm steam partial pressure at 1100 K

of steam partial pressure on the overall yield of fluxes of product gases.

Generally, increasing the partial pressure of steam from 0.1 to 0.2 atm, the rate of steam gasification reaction (R1) is almost double which produces more hydrogen and carbon monoxide (Prestipino et al. 2018). The carbon monoxide is further reacted with steam (R5) to form more hydrogen and carbon dioxide causing an increase of hydrogen fluxes 1.8-fold compared to that at 0.1 atm partial pressure of steam (Fig. 8). Due to lower reaction temperature (1100 K), less increments in the carbon monoxide flux is observed. Overall, the high yield of H_2 can be achieved at high steam partial pressure.

Effect of particle size

The particle sizes of 5 and 10 mm are used for the gasification process at the reaction temperature of 1100 K with steam partial pressure of 0.2 atm. The individual gas (H_2 , CO, CO_2) flux ratio with respect to time at 1100 K temperature and 0.2 atm partial pressure are represented in Fig. 9.

Generally, the overall rate of conversion of char particle increases with a decrease in the particle size. In a gasification process with smaller particle, the steam diffuses deep in the char particle and reactions continue throughout the particle following the progressive model. While, in case of large particle, reactions take place at the outer surface of the particle and steam does not reach deep into the particle follow the shrinking core model (Yadav and Kumar 2016). Hence, the rate of the surface reaction of large char particle is high as compared to the small particle causing six to eight-fold increase in CO production rate. This leads to higher overall fluxes of product gas for large size particle and lower for small size particle.

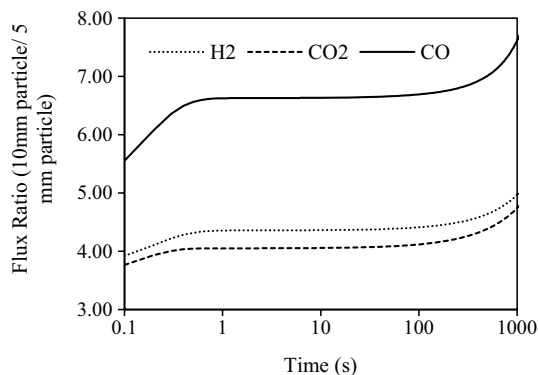


Fig. 9 Ratio of overall molar fluxes of H_2 , CO_2 and CO from outer surface of particle from 10 to 5 mm particle size at 1100 K with steam partial pressure of 0.2 atm

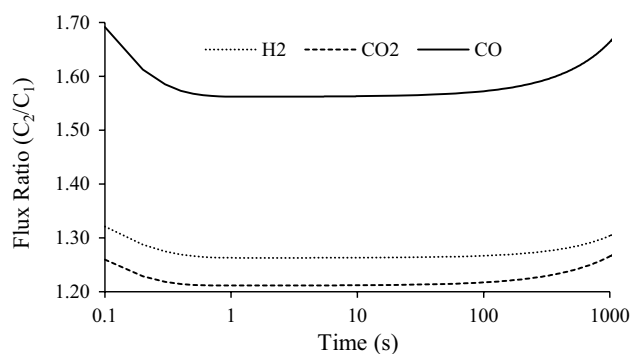


Fig. 10 Ratio of overall molar fluxes of H_2 , CO_2 and CO from outer surface of particle with 158 and 100 kmol/m^3 carbon concentrations in the particle at 1100 K with steam partial pressure of 0.2 atm

Effect of carbon concentration

The char particle (10 mm) with variable carbon concentration of C_1 -100 and C_2 -158 kmol/m^3 are used for this study. The concentration variation may be caused due to internal porosity of the char particle. The variation of carbon flux ratio (C_2/C_1) of different product gases (H_2 , CO , CO_2) with respect to time at 1100 K temperature and 0.2 atm partial pressure is shown in Fig. 10.

The consumption of carbon near the surface of the char particle during gasification is more for a higher carbon concentration, but for lower carbon concentration of char, the consumption of carbon is higher towards the centre of the particle because of diffusivity. Owing to this reason, the overall fluxes of product gas are higher for larger carbon concentration of char particle.

Overall, the high CO and H_2 concentration is desirable properties of syngas and its concentration in the product gas may depend upon the physical and chemical properties of solid fuel and the operating conditions used in the gasification process. The use of mathematical model may be helpful in the prediction of output gases and input, output parameters easily correlated.

Conclusion

In this study, an unsteady state mathematical model for the production of synthesis gas using steam gasification process is developed. By which the effect of reaction temperature, particle size, steam partial pressure and carbon concentration in the char particle on the gasification process are studied. This study reveals that the highest concentration of CO and H_2 and minimum fraction of CO_2 in the synthesis gas are obtained when the reaction temperature is greater than 1200 K (lesser time, < 600 s). In addition, the present model deals with that and also, it is analysed

that the removal of the ash layer from the particle surface at the gasification time of 100 s may give higher CO concentration. The high H_2 concentration may be achieved by maintaining high steam partial. The opposite relationships are obtained between the rate of conversion and particle size while the fluxes of product gas are varying with particle size.

Acknowledgements The authors gratefully acknowledge the financial and other related support from Indian Institute of Technology Roorkee, India.

References

- Chandra A, Chandra H (2004) Impact of Indian and imported coal on Indian thermal power plants. *J Sci Ind Res India* 63:156–162
- Chavan P, Datta S, Saha S, Sahu G, Sharma T (2012) Influence of high ash Indian coals in fluidized bed gasification under different operating conditions. *Solid Fuel Chem* 46:108–113
- Chen J, Chen W, Ji R, Jiao Y, Wang X (2019) Kinetic studies on bituminous coal char gasification using CO_2 and H_2O mixtures. *Int J Green Energy* 16:1144–1151
- Choudhary D, Shankar R (2012) An STEEP-fuzzy AHP-TOPSIS framework for evaluation and selection of thermal power plant location: a case study from India. *Energy* 42(1):510–521
- Corella J, Sanz A (2005) Modeling circulating fluidized bed biomass gasifier. A pseudo-rigorous model for stationary state. *Fuel Process Technol* 86:1021–1053
- Everson RC, Neomagus HWJP, Kasaini H, Njapha D (2006) Reaction kinetics of pulverized coal-chars derived from inertinite-rich coal discards: characterisation and combustion. *Fuel* 85:1067–1075
- Gil S, Mocek P, Bialik W (2011) Changes in total active centres on particle surfaces during coal pyrolysis, gasification and combustion. *Chem Eng Process* 32:155–169
- Gomez A, Mahinpey N (2015) Kinetic study of coal steam and CO_2 gasification: a new method to reduce interparticle diffusion. *Fuel* 148:160–167
- Gomez-Barea A, Ollero P (2006) An approximate method for solving gas–solid non-catalytic reactions. *Chem Eng Sci* 61:3725–3735
- Groeneveld MJ, Swaaij WPMV (1980) Gasification of char particles with CO_2 and H_2O . *Chem Eng Sci* 35:307–313
- Hecht ES, Shaddix CR, Geier M, Molina A, Haynes BS (2012) Effect of CO_2 and steam gasification reactions on the oxy-combustion of pulverized coal char. *Combust Flame* 159(11):3437–3447
- Holikova K, Zajdlík R, Markos J, Jelemensky L (2005) Comparison of single coal char particle combustion at different conditions. *Chem Pap* 59:413–420
- Inayat A, Ahmad MM, Yusup S, Mutalib MIA (2010) Biomass steam gasification with in-situ CO_2 capture for enriched hydrogen gas production: a reaction kinetics modelling approach. *Energies* 3:1472–1484
- Jayaraman K, Gökulp I, Jeyakumar S (2017) Estimation of synergetic effects of CO_2 in high ash coal-char steam gasification. *Appl Therm Eng* 110:991–998
- Kajitani S, Suzuki N, Ashizawa M, Hara S (2006) CO_2 gasification rate analysis of coal char in entrained flow coal gasifier. *Fuel* 85:163–169
- Kwon TW, Kim SD, Fung DPC (1988) Reaction kinetics of char- CO_2 gasification. *Fuel* 67:530–535

- Lahijani P, Zainal ZA, Mohammadi M, Mohamed AR (2015) Conversion of the greenhouse gas CO₂ to the fuel gas CO via the Boudouard reaction: a review. *Renew Sustain Energy Rev* 41:615–632
- Li Z, Yang T, Yuan S, Yin Y, Devid EJ, Huang Q, Auerbach D, Kleyn AW (2020) Boudouard reaction driven by thermal plasma for efficient CO₂ conversion and energy storage. *J Energy Chem* 45:128–134
- Luo C, Watanabe T, Nakamura M, Uemiya S, Kojima T (2001) Development of FBR measurement of char reactivity to carbon dioxide at elevated temperatures. *Fuel* 80:233–243
- Mendes A, Dollet A, Ablitzer C, Perrais C, Flamant G (2008) Numerical simulation of reactive transfer in spouted beds at high temperature: application to coal gasification. *J Anal Appl Pyrolysis* 82:117–128
- Mermoud F, Gollfer F, Salvador S, de Steene LV, Dirion JL (2006) Experimental and numerical study of steam gasification of a single charcoal particle. *Combust Flame* 145:59–79
- Mishra A, Gautam S, Sharma A (2018) Effect of operating parameters on coal gasification. *Int J Coal Sci Technol* 5:113125
- Mohamad AA (2005) Combustion in porous media: fundamentals and applications. *Transport phenomena in porous media III*. Elsevier, Pergamon, pp 287–304
- Prabhakar A, Sadhukhan AK, Bhunia S, Gupta P (2019) Modelling and experimental investigations on gasification of coarse sized coal char particle with steam. *J Energy Inst* 92:1502–1518
- Prestipino M, Galvagno A, Karlström O, Brink A (2018) Energy conversion of agricultural biomass char: steam gasification kinetics. *Energy* 161:1055–1063
- Seshadri K, Bai XS (2017) Rate-ratio asymptotic analysis of the influence of addition of carbon monoxide on the structure and mechanisms of extinction of nonpremixed methane flames with comparison to experiments. *Combust Flame* 175:107–117
- Shufen L, Ruizheng S (1994) Kinetic studies of a lignite char pressurized gasification with CO₂, H₂ and steam. *Fuel* 73:413–416
- Tremel A, Spliethoff H (2013) Gasification kinetics during entrained flow gasification—Part II: intrinsic char reaction rate and surface area development. *Fuel* 107:653–661
- Umeki K, Yamamoto K, Namioka T, Yoshikawa K (2010) High temperature steam-only gasification of woody biomass. *Appl Energy* 87:791–798
- Varma AK, Thakur LS, Shankar R, Mondal P (2019) Pyrolysis of wood sawdust: effects of process parameters on products yield and characterization of products. *Waste Manag* 89:224–235
- Wang X, Jiang M, Yao Y, Zhang Y, Cao J (2009) Steam gasification of coal char catalyzed by K₂CO₃ for enhanced production of hydrogen without formation of methane. *Fuel* 88:1572–1579
- Wang ZH, Zhang K, Li Y, He Y, Kuang M, Li Q, Cen KF (2016) Gasification characteristics of different rank coals at H₂O and CO₂ atmospheres. *J Anal Appl Pyrol* 122:76–83
- Xu Q, Pang S, Levi T (2011) Reaction kinetics and producer gas compositions of steam gasification of coal and biomass blend chars, part 2: mathematical modelling and model validation. *Chem Eng Sci* 66:2232–2240
- Yadav VK, Kumar V (2014) Modelling gasification of single coal particle. In: 5th International and 41th National conference on fluid mechanics and fluid power (FMFP-2014), 12th–14th December 2014, IIT Kanpur
- Yadav VK, Kumar V (2016) Staggered grid finite volume approach for modeling single particle char gasification. *Int J Chem React Eng* 14(3):749–756
- Ye DP, Agnew JB, Zhang DK (1998) Gasification of a South Australian low-rank coal with carbon dioxide and steam: kinetics and reactivity studies. *Fuel* 77:1209–1219
- Zajdlík R, Jelemenský L, Markos J, Remiarová B (2001) Modelling of gasification of a single coal char particle. *Chem Pap* 55:364–368
- Zeng DW, Xiao R, Zhang S, Zhang HY (2015) Bio-oil heavy fraction for hydrogen production by iron-based oxygen carrier redox cycle. *Fuel Process Technol* 139:1–7
- Zeng J, Xiao R, Zeng D, Zhao Y, Zhang H, Shen D (2016) High H₂/CO ratio syngas production from chemical looping gasification of sawdust in a dual fluidized bed gasifier. *Energy Fuel* 30(3):1764–1770
- Zhu L, Wang Y, Zhang Z, Li J, Yu G (2020) Effects of H₂ and CO on char-gasification reactivity at high temperatures. *Energy Fuel* 34:720–727

Publisher's Note Springer Nature remains neutral with regard to jurisdictional claims in published maps and institutional affiliations.